© 2021. Published by The Company of Biologists Ltd | Journal of Experimental Biology (2021) 224, jeb242496. doi:10.1242/jeb.242496

RESEARCH ARTICLE

The relationship between myonuclear number and protein synthesis in individual rat skeletal muscle fibres

Satoru Ato[1,2,*] and Riki Ogasawara[1,*]

ABSTRACT

Skeletal muscle has numerous nuclei within a cell. The nucleus is considered as the central organelle for muscle protein synthesis (MPS). However, it is unclear whether myonuclear number is associated with MPS capacity within the individual muscle fibres. Therefore, the purpose of the present study was to reveal the relationship between myonuclear number per unit muscle fibre length and MPS under basal and conditions of elevated MPS by high-intensity muscle contraction (HiMC) using an *in vivo* nascent protein labelling technique (SUnSET) in rodents. We found that myonuclear number was positively correlated with MPS in individual muscle fibres in the basal condition. Similarly, ribosomal protein S6 (rpS6) content, which is a rough estimate of ribosome content, was positively correlated with MPS. However, myonuclear number was not associated with rpS6 content. In contrast to the basal condition, when MPS was increased by acute HiMC, no correlation was observed between myonuclear number and MPS, but the association between rpS6 and MPS was maintained. Importantly, these observations indicate that the number of nuclei in individual myofibers is related only to MPS at rest. However, the ribosome content in individual fibres is related to MPS of individual myofibers both at rest and following HiMC.

KEY WORDS: Myonuclei, Muscle contraction, Protein synthesis

INTRODUCTION

Skeletal muscle is an essential motor organ in various animals. Skeletal muscles undergo significant changes in muscle mass and function in response to changes in the external environment and other stimuli. The balance between protein synthesis and breakdown within skeletal muscle cells is considered to play an important role in the regulation of skeletal muscle cell size. Both muscle protein synthesis (MPS) and muscle protein breakdown (MPB) change during atrophy and hypertrophy, but the changes in MPS are greater than those in MPB. Thus, protein synthesis is considered the key determinant of skeletal muscle mass (Goodman et al., 2011a; Ogasawara et al., 2016; You et al., 2015).

Mature skeletal muscle cells function as syncytia, which are fused by multiple muscle progenitors during development (Lepper et al., 2011; Sambasivan et al., 2011). This generates skeletal muscle fibres with numerous nuclei within each cell. The reason mature skeletal muscle forms syncytia is unclear. The myonuclear number within cells has been strongly correlated with skeletal muscle cell size *in vivo* (Allen et al., 1995; Ato et al., 2019; Roy et al., 1999). Moreover, myonuclear number increases through the differentiation of skeletal muscle stem cells, concomitant with muscle hypertrophy due to intense muscle contraction, such as in mechanical overload and resistance training. The extent of the increase in myonuclear number by resistance training is positively associated with muscle hypertrophy (Ato et al., 2019; Snijders et al., 2016). The nucleus plays a central role in protein synthesis via ribosome synthesis and mRNA supply (Hall and Ralston, 1989; Thomson et al., 2013). Thus, myonuclear number is probably associated with MPS capacity at rest or during increased protein synthesis caused by muscle hypertrophic stimuli such as intense muscle contraction (Gundersen, 2016; Petrella et al., 2008). However, it is technically difficult to assess protein synthesis and the number of myonuclear cells within a single muscle fibre. Consequently, the relationship between the number of myonuclei and the ability to synthesise muscle proteins has not yet been clarified.

Approaches to labelling newly synthesised proteins using isotopic labelling techniques (e.g. radioisotopes and stable isotopes) have been used for half a century. These approaches have revealed the protein synthetic response *in vivo* (Anthony et al., 2000; Morkin, 1970). Puromycin is a structural analogue of tyrosyl-tRNA, and it can be incorporated into the elongating nascent polypeptide via a peptide bond under very low doses and with a short exposure period, without inducing any stress response (Schmidt et al., 2009). Thus, puromycin-based nascent polypeptide labelling (the *in vivo* SUnSET technique) has been established as a convenient and reliable means to monitor protein translation using both biochemical and histochemical assays (Goodman et al., 2011b; Liu et al., 2012; Schmidt et al., 2009), and is widely used in various tissues and species (Enam et al., 2020; Goodman et al., 2011b; Ravi et al., 2018). This technique allows the evaluation of the synthesised protein per unit time and myonuclear number in a muscle fibre simultaneously. Therefore, we aimed to reveal the relationship between myonuclear number and protein synthesis within a single myofiber by applying the *in vivo* SUnSET technique under resting and increased MPS conditions due to intense muscle contraction.

MATERIALS AND METHODS

Animals

The study protocol was approved by the Ethics Committee for Animal Experiments at Nagoya Institute of Technology (Nagoya, Japan). Ten week old male Sprague–Dawley rats were purchased from Japan SLC (Hamamatsu, Japan). The rats were acclimatised in an environmental room maintained at 22°C with an alternating 12 h light–dark cycle. Food and water were available *ad libitum* until the experiments began.

High-intensity muscle contraction

High-intensity muscle contraction (HiMC) was performed using our previously described rodent resistance exercise model

[1]Department of Life Science and Applied Chemistry, Nagoya Institute of Technology, Showa-ku, Nagoya 466-8555, Japan. [2]Japan Society for the Promotion of Science, Kojimachi Business Center Building, 5-3-1 Kojimachi, Chiyoda-ku, Tokyo 102-0083, Japan.

*Authors for correspondence (satorugby@gmail.com; ogasawara.riki@niteh.ac.jp)

S.A., 0000-0002-0667-8790; R.O., 0000-0002-2600-1613

Received 3 March 2021; Accepted 7 April 2021

Journal of Experimental Biology (2021) 224, jeb242496. doi:10.1242/jeb.242496

(Ogasawara et al., 2016), with some modification. The original method elicited muscle contraction in the gastrocnemius muscle. In the present study, the tibialis anterior (TA) muscle was used because it has more fast muscle fibre than the gastrocnemius muscle. After an overnight fast, the hair of the lower legs of each rat was removed under inhaled isoflurane anaesthesia. The rats were placed in the prone position, and the right lower leg was held on the footplate to generate a tibia–foot angle of 120 deg. Disposable surface electrodes were placed to cover the TA muscle. Electrical stimulation was performed on the right lower leg similar to that performed in our previous model (10 contractions of 3 s duration, with a 7 s interval between contractions for five sets, with 3 min rest intervals). Stimulation frequency (100 Hz) and voltage (∼30 V) were set to produce maximal tetanic force. The contralateral non-stimulated left leg served as the control. After acute muscle contraction, the rats were monitored until they awoke and were returned to their cages. The rats were killed 6 h after muscle contraction by the removal of blood from the ventral aorta under inhaled isoflurane anaesthesia. The TA muscles of both legs were removed and divided into three pieces for biochemical and histochemical analyses. In detail, the whole TA muscle was cut into two parts at the middle of its long-side length. The piece on the insertion side was frozen in liquid nitrogen-cooled isopentane embedded with OCT compound. The piece on the origin side was divided into two parts at the middle of its short side. One piece was frozen in liquid nitrogen for western blotting; the other was frozen in liquid nitrogen-cooled isopentane for single fibre isolation. The samples were stored at −80°C until analysis.

In vivo SUnSET

In vivo SUnSET was performed as previously described (Goodman et al., 2011b). Briefly, puromycin (0.04 µmol g^{-1} body mass; FUJIFILM Wako Pure Chemical Corporation, Tokyo, Japan; diluted in 0.02 mol l^{-1} phosphate-buffered saline, PBS) was injected intraperitoneally under anaesthesia 15 min before exsanguination (see above).

Western blot

The powdered frozen muscle was homogenised with 10 volumes of ice-cold radioimmunoprecipitation buffer. The homogenate was then centrifuged at 2000 ***g*** for 3 min at 4°C. The resulting supernatant was collected, and the protein concentration was measured using the Protein Assay Rapid Kit Wako II (FUJIFILM Wako Pure Chemical Corporation). The supernatant was mixed with 3× sodium dodecyl sulphate (SDS) sample buffer and heated at 95°C for 5 min. The sample (20 µg protein) was resolved by SDS-PAGE using a 10% gel, and the proteins were transferred to a ClearTrans® polyvinylidene fluoride membrane (FUJIFILM Wako Pure Chemical Corporation). The membrane was blocked with Bullet Blocking One for Western Blotting (Nacalai Tesque, Kyoto, Japan). After three washes with Tris-buffered saline containing 0.1% TWEEN® 20 (TBST), the membrane was incubated with mouse anti-puromycin monoclonal antibody (mAb, cat. no. MABE 343, Merck, Darmstadt, Germany) at 4°C overnight. The following day, the membrane was washed using TBST and incubated with a secondary antibody for 90 min at room temperature. After three washes with TBST, the membrane was incubated with Immobilon Forte Western HRP substrate (Merck), and chemiluminescence was detected using a ChemiDoc XRS+ (Bio-Rad Laboratories, Hercules, CA, USA). Protein band intensity was measured using Image Lab™ 6.0.1 (Bio-Rad) and normalised to a Coomassie Blue-stained total protein band.

Immunofluorescence of muscle cross-sections

The sample was transversely sectioned at a thickness of 8 µm in a cryostat at −22°C (OTF 5030, Bright Instruments, Luton, UK). Sections were placed on MAS-coated glass slides (Matsunami Glass, Kishiwada, Japan) and rapidly fixed in 4% paraformaldehyde (PFA) in PBS for 10 min. After three 5 min washes with PBS, the sections were incubated with blocking buffer (5% goat serum in 0.3% Triton X-100/PBS, PBS-T) for 30 min at room temperature. After washing 3 times with PBS, the sections were incubated with mouse anti-puromycin mAb diluted 1:100 in 1% bovine serum albumin (BSA) in PBS-T at 4°C overnight. The following day, the sections were incubated with diluted Alexa Fluor® 488-conjugated goat anti-mouse IgG, $F(ab')_2$ fragment (Cell Signaling Technology, Danvers, MA, USA) for 90 min at room temperature. The TA muscle sections from a rat that was not treated with puromycin were used to distinguish tissue autofluorescence and puromycin-derived fluorescence. Then, the sections were counter-stained with CF®350 dye-conjugated wheat germ agglutinin (WGA, Biotium, Fremont, CA, USA) to visualise the cell membrane. Glass slides were washed with PBS and mounted with Vectashield® Antifade Mounting Medium (Vector Laboratories, Burlingame, CA, USA). The sections were visualised with a semiapochromat (FL) 20×/0.45NA objective on a fluorescence microscope (IX73, Olympus, Tokyo, Japan) equipped with a global shutter CMOS camera (AdvanCam-E3RGc, AdvanVision, Tokyo, Japan). The exposure time and gain were set to avoid fluorescence signals in a control slide that was not treated with primary antibody and for samples from a rat that was not treated with puromycin. Five points per section (which contains 215–284 fibres) were captured randomly and the average pixel intensity within the fibres was measured with ImageJ 1.53c software (NIH, Bethesda, MD, USA). The fibres on the border and edge were excluded from the analysis. Representative wide-view tiled images (Fig. 2C) were taken using an LSM 880 microscope (Carl Zeiss, Oberkochen, Germany).

Single skeletal muscle fibre isolation and immunofluorescence

Mechanical single fibre isolation from frozen muscle was performed as previously described (Donaldson, 1984) with some modifications. We chose this approach because the original technique has the advantage of excluding the non-muscle nucleus (Konigsberg et al., 1975; Roy et al., 1999). In detail, 50% glycerol containing 100% relaxing solution supplemented with protease inhibitor (Halt™ Protease Inhibitor Cocktail, Thermo Fisher Scientific, Waltham, MA, USA) was pre-cooled to −20°C. A frozen piece of TA muscle was immersed in the solution and gradually thawed by increasing the temperature of the chamber from −20 to 0°C overnight. The thawed muscle was transferred to ice-cold 100% relaxing solution containing protease inhibitor. Single skeletal muscle fibres were dissected using fine forceps. These isolated fibres were rapidly fixed for 10 min in 4% PFA in PBS at room temperature and then washed 3 times in PBS (5 min each wash). Muscle fibres were then collected in a 1.5 ml tube using a Pasteur pipette. Permeabilisation and blocking were performed in 1% Triton X-100 and 5% goat serum in PBS for 30 min at room temperature with gentle shaking. After three PBS washes, the muscle fibres were incubated with mouse anti-puromycin mAb diluted 1:100 and rabbit anti-PCM1 polyclonal antibody (cat. no. HPA023370, Sigma, St Louis, MO, USA) diluted 1:100, mouse anti-fast myosin mAb (cat. no. M4276, Sigma) diluted 1:100 and rabbit anti-ribosomal protein S6 (rpS6) mAb (cat. no. 2217, Cell Signaling Technology) diluted 1:100, or mouse anti-puromycin mAb diluted 1:100 and rabbit anti-rpS6 mAb diluted 1:100 at 4°C overnight with gentle shaking. The diluent was 1% BSA and 0.3%

Triton X-100 in PBS. The antigen–antibody reaction on the slide did not allow the antibody to penetrate deep into the fibres, even after two overnight reactions, suggesting that flotation and shaking methods are necessary steps to allow the primary antibody to penetrate deeply. After overnight incubation, the muscle fibres were washed and incubated with Alexa Fluor® 488-conjugated goat anti-mouse IgG F(ab′)$_2$ fragment and Alexa Fluor® 555-conjugated goat anti-rabbit IgG F(ab′)$_2$ fragment (Cell Signaling Technology) in antibody diluent at 4°C overnight with gentle shaking. The muscle fibres were washed and placed on a MAS-coated glass slide and mounted with Vectashield® Antifade Mounting Medium with DAPI (4′,6-diamidino-2-phenylindole, Vector Laboratories). DAPI was used to visualise all nuclei attached to the muscle fibres. The verification of puromycin-derived fluorescence was carried out using muscle fibres from a rat that was not treated with puromycin, as a negative control (see Fig. 1B). The other antibodies were validated for reactivity by reacting only with the secondary antibodies.

Confocal microscopy and data acquisition

Isolated muscle fibres [puromycin/PCM1 labelled: 173 fibres in total from four non-contracted (87 fibres) and HiMC-subjected (86 fibres) legs of rats, 17–29 fibres per leg; puromycin/rpS6 labelled: 149 fibres in total from four non-contracted (73 fibres) and HiMC-subjected (76 fibres) legs of rats, 23–30 fibres per leg] were filmed using a Plan-Apochromat 40×/1.4 NA and 63×/1.4 NA oil immersion objective on a model LSM 880 confocal laser microscope (Carl Zeiss). For quantitative measurement, anti-puromycin/anti-PCM1 antibody-labelled fibres, and anti-puromycin/anti-rpS6 antibody-labelled fibres were filmed using a z-stack at 1 µm intervals. Fluorescence was emitted by an argon laser for Alexa Fluor® 488 and by a diode laser for DAPI and Alexa Fluor® 555. Fluorescence signals and phase contrast images were simultaneously obtained. Airy disc size was set such that the optical section thickness was 2 µm. Three points were selected at random and photographed per fibre. The ends of the fibres and neuromuscular junction-like regions with dense nuclei were excluded. z-Stack images were averaged, and puromycin-derived fluorescence intensity was measured using ImageJ 1.53c software (NIH). The length of a muscle fibre was determined by extracting the edge of the fibre, delineating it, and averaging the length of this delineation on both sides of the fibre. The average length of 10 sarcomeres obtained from the phase contrast image was used as the sarcomere length. The myofiber cross-sectional area (CSA) was determined by obtaining orthogonal images of the *y*–*z* axis from the z-stack images of puromycin and creating a binary image. PCM1-positive nuclei were manually counted using the cell counter plugin in ImageJ and used as the myonuclear number. In this study, all the nucleus labeled with DAPI in individual muscle fibres was PCM1 (a myonuclear marker; Winje et al., 2018) positive, indicating that the non-muscle nuclei were efficiently removed.

Statistical analysis

Paired *t*-test was used to determine the effect of HiMC on MPS, rpS6 content and myonuclear number. Pearson's correlation coefficient was used to compare the relationship between myonuclear number, fibre CSA, rpS6 content and MPS. Statistical analysis was performed with JMP® Pro 14 (SAS Institute, Cary, NC, USA). Statistical significance was set at $P<0.05$.

RESULTS

Characteristics of puromycin-labelled single muscle fibres

First, we confirmed the structural integrity of isolated muscle fibres by visualisation of myosin and rpS6 (Fig. 1A). Sarcomeric striation was evident by myosin labelling. In addition, rpS6 was observed around the nucleus and in an alternating pattern with that of myosin (A-band), suggesting that ribosomes are abundantly located around the I-band. Second, we observed anti-puromycin antibody-labelled protein in isolated single fibres. Puromycin fluorescence in an isolated muscle fibre (Fig. 1B, top) was abundant as compared with the negative control (TA muscle fibre obtained from rat that was not treated with puromycin). The puromycin fluorescence pattern was similar to that of rpS6 (Fig. 1C). In addition, we confirmed that puromycin and rpS6 were labelled deep into the fibres, by z-stack imaging (Fig. 1D,E).

Effect of acute HiMC on MPS in TA muscle

The increase in protein synthesis in TA muscle following acute HiMC was confirmed by western blotting (Fig. 2A,B), and immunostaining of a muscle cross-section (Fig. 2C,D) and isolated muscle fibres (Fig. 2E,F). Myonuclear number (PCM1-positive nucleus) was unchanged after acute HiMC; furthermore, rpS6 content within the fibres was also unaltered by acute HiMC (Fig. 4A,B).

Relationship between myonuclear number per unit fibre length, ribosome content and MPS under basal and elevated MPS due to acute HiMC

Myonuclear number per 200 µm fibre length was positively correlated with MPS in muscle fibres from control legs (Fig. 3A; $r=0.2852$, $P<0.01$). However, the correlation was not observed in muscle fibres from legs subjected to HiMC treatment (Fig. 3B; $r=-0.0288$, $P=0.7925$).

Myonuclear number per unit fibre length did not correlate with rpS6 content, either in the control legs (Fig. 3C; $r=0.1813$, $P=0.1244$) or legs subjected to HiMC treatment (Fig. 3D; $r=0.0165$, $P=0.1394$). However, rpS6 content was significantly correlated with MPS, both in the control legs (Fig. 3E; $r=0.5272$, $P<0.01$) and in legs subjected to HiMC treatment (Fig. 3F; $r=0.4836$, $P<0.01$).

Relationship between myofiber CSA and number of myonuclei, ribosome content and MPS

Finally, we evaluated the relationship between the number of myonuclei and muscle fibre CSA, and the possible mediating factors, MPS and ribosome volume. The myonuclear number per unit fibre length was positively correlated with individual myofiber CSA (Fig. 4A; $r=0.3302$, $P<0.01$). However, the basal MPS within myofibers was inversely correlated with myofiber CSA (Fig. 4B; $r=-0.3825$, $P<0.01$). Furthermore, basal rpS6 content was not associated with individual myofiber CSA (Fig. 4C; $r=-0.2042$, $P=0.0831$).

DISCUSSION

The relationship between myonuclear number and MPS in single muscle fibres was explored at the basal level and with elevated MPS due to HiMC by visualising myonuclear and synthesised protein simultaneously using the *in vivo* SUnSET. Our main finding was that the myonuclear number per unit fibre length was weakly correlated with basal MPS but not with HiMC-induced elevated MPS. In addition, myonuclear number per unit fibre length was not correlated with rpS6 content, whereas rpS6 content was consistently correlated positively with MPS in individual muscle fibres both at rest and with elevated MPS due to HiMC. Furthermore, the number of myonuclei was positively correlated with myofiber size. However, MPS was negatively associated with myofiber size, even though it was weakly but significantly correlated with the number of myonuclei.

Journal of Experimental Biology (2021) 224, jeb242496. doi:10.1242/jeb.242496

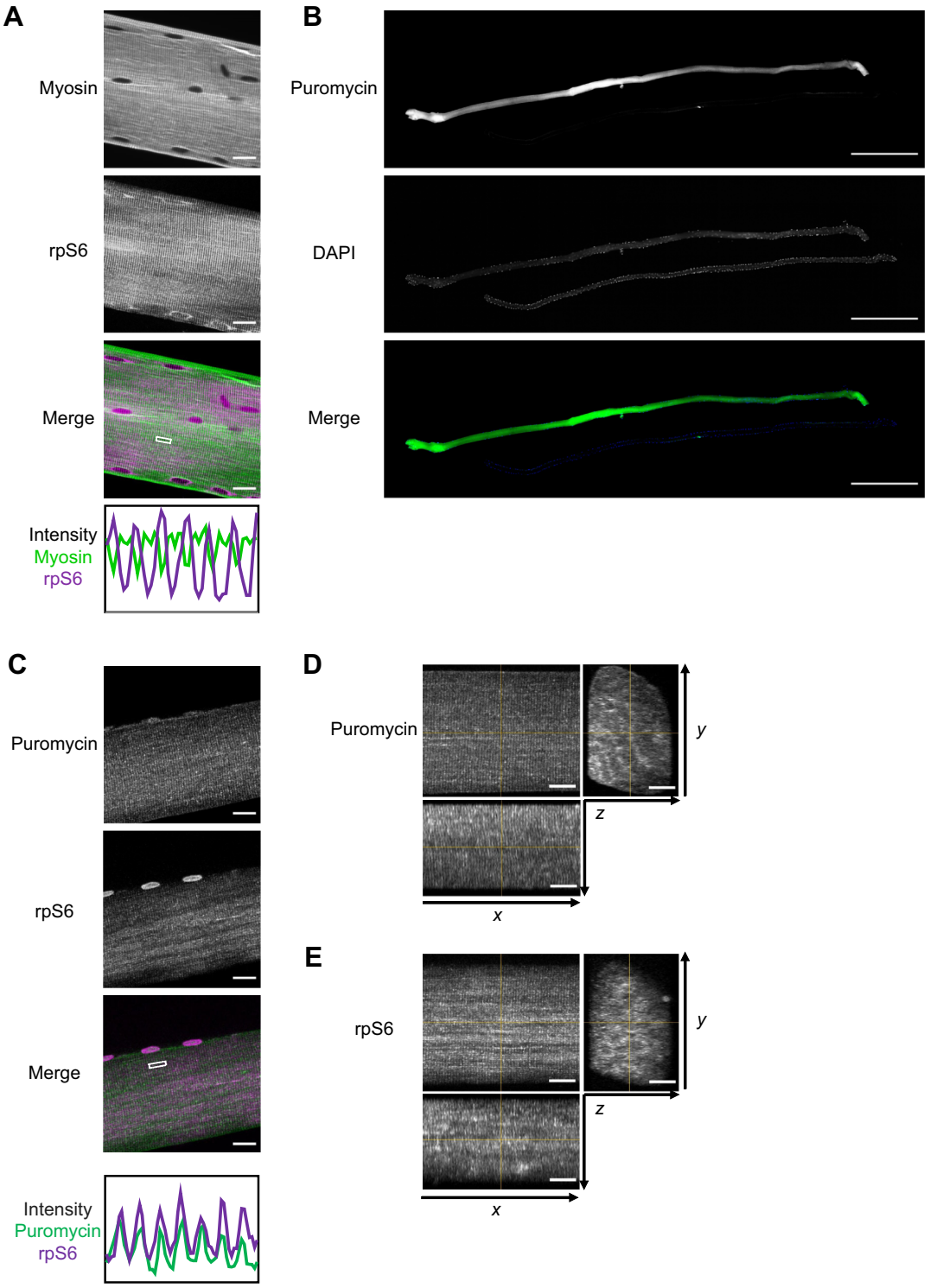

Fig. 1. Morphological integrity of isolated muscle fibres from freeze-thawed skeletal muscle. (A) Image of an isolated myofiber labelled with anti-rabbit ribosomal protein S6 antibody (rpS6; magenta in merge) and anti-mouse myosin antibody (green in merge). Fluorescence intensity profiles were obtained from the regions of interest (ROI) surrounded by dashed squares within merge image. Scale bars: 20 μm. (B) Comparison of anti-puromycin antibody-labelled (green; top side in the picture) isolated myofiber and the negative control (muscle fibre from a rat not treated with puromycin; bottom side in the picture). Each fibre was counterstained with DAPI (blue). Scale bars: 1 mm. (C) Image of an isolated myofiber labelled with anti-puromycin antibody (green) and rpS6 (magenta). Fluorescence intensity profiles were obtained from the ROI surrounded by dashed squares within merge image. Scale bars: 20 μm. (D) Orthogonal projection image (*x*–*y*, *x*–*z* and *y*–*z*) of puromycin expression in an isolated muscle fibre. Scale bars: 20 μm. (E) Orthogonal projection image (*x*–*y*, *x*–*z* and *y*–*z*) of rpS6 in an isolated muscle fibre. Scale bars: 20 μm.

Glycerol-immersed muscle-derived isolated muscle fibres were used in this study. This method was originally described by Donaldson (1984) and has the advantage of excluding non-muscle cells without affecting immunoreactivity (Konigsberg et al., 1975; Roy et al., 1999). An alternating pattern of rpS6 and myosin according to sarcomere striation was observed (Fig. 1A). Several

Journal of Experimental Biology (2021) 224, jeb242496. doi:10.1242/jeb.242496

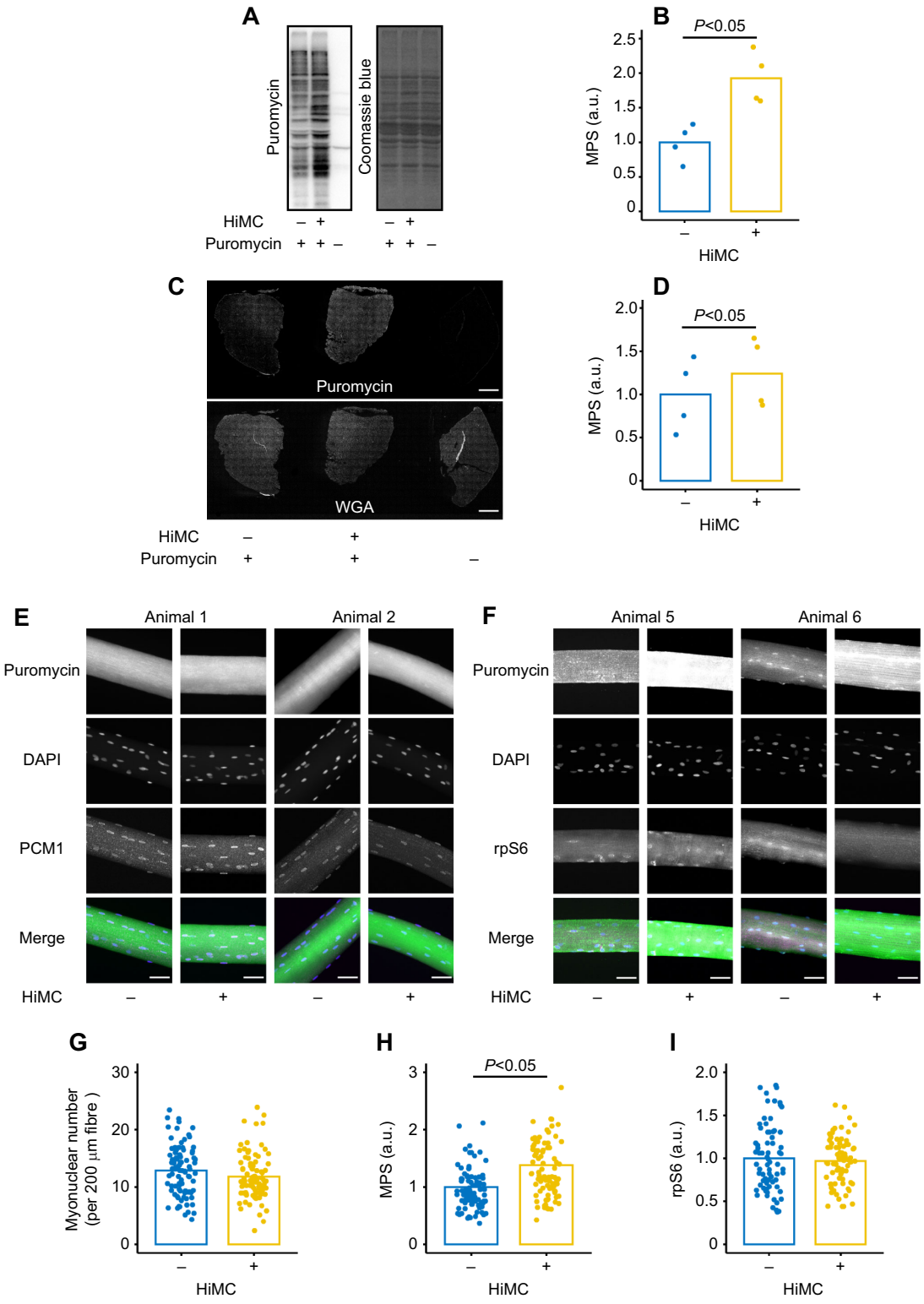

Fig. 2. Effect of acute high-intensity muscle contraction (HiMC) on muscle protein synthesis (MPS) in the tibialis anterior (TA) muscle. (A) Representative western blot of puromycin-labelled protein expression with and without HiMC. (B) MPS (a.u., arbitrary units) measured in TA muscle homogenates by western blot with and without HiMC (n=4). (C) Anti-puromycin antibody-labelled TA muscle cross-section. All sections were counter-stained with wheat germ agglutinin (WGA) to visualise the tissue outline. Scale bars: 2 mm. (D) MPS measured from a muscle cross-section via immunofluorescence with and without HiMC (n=4). (E) Anti-puromycin (green in merge) and anti-PCM1 (magenta in merge) antibody-labelled isolated myofibers from non-contracted legs and legs subjected to HiMC. Nuclei were stained with DAPI (blue in merge). Scale bars: 20 μm. (F) Anti-puromycin (green) and anti-rpS6 (magenta) antibody-labelled isolated myofibers from non-contracted legs and legs subjected to HiMC. Nuclei were stained with DAPI (blue). Scale bars: 20 μm. (G) Influence of acute HiMC on the number of PCM1-positive nuclei per 200 μm fibre length. (H) Effect of acute HiMC on MPS in isolated muscle fibres. (H) Effect of acute HiMC on rpS6 content in isolated muscle fibres. Means and individual values are expressed using a bar and dot plot. Statistical analysis was performed with paired t-tests.

Journal of Experimental Biology (2021) 224, jeb242496. doi:10.1242/jeb.242496

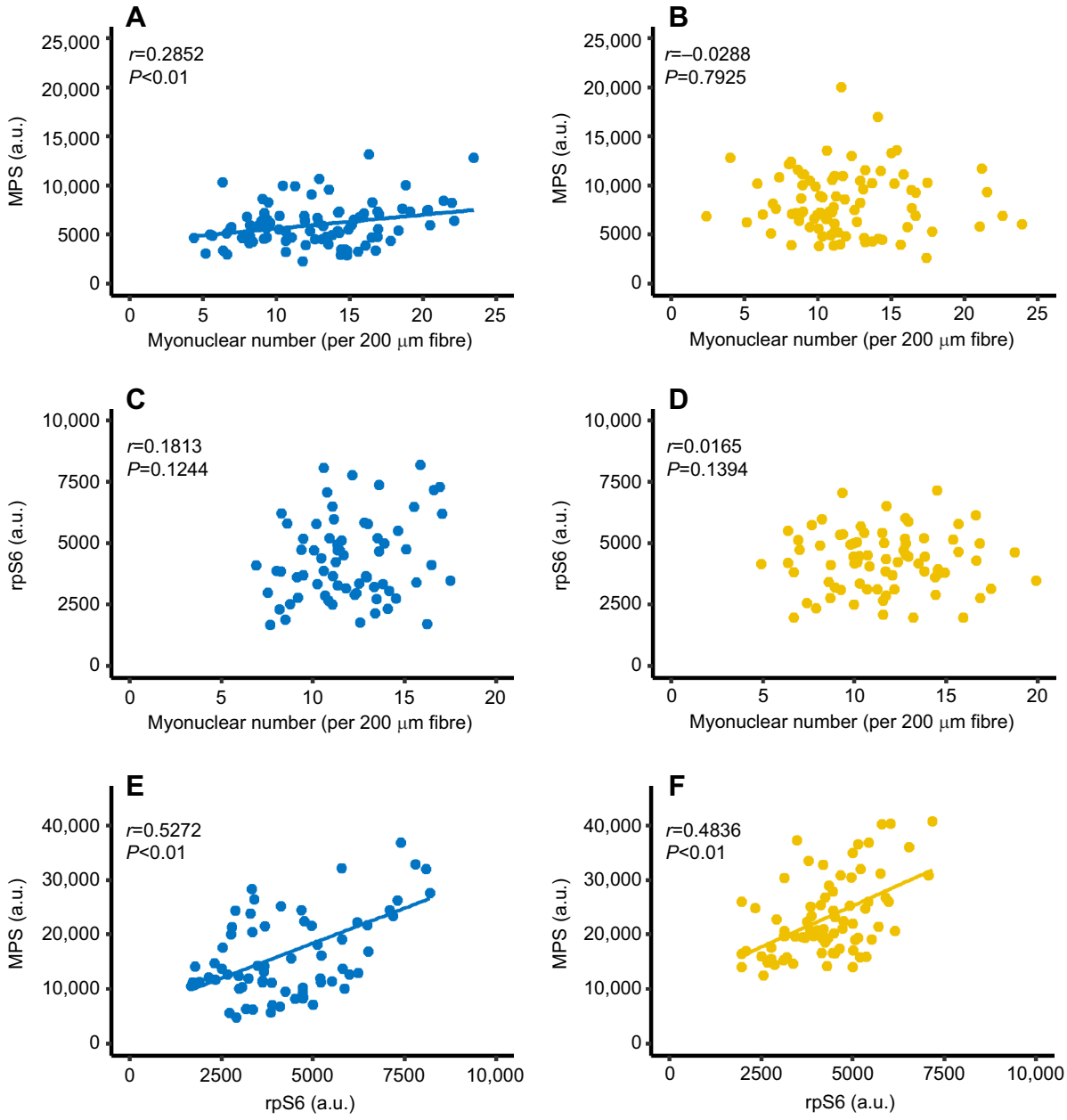

Fig. 3. Relationship between myonuclear number per unit fibre length, ribosome content and MPS under basal and elevated MPS due to acute HiMC. (A,B) Relationship between myonuclear number and MPS in individual myofibers from non-contracted legs (basal; A) and legs subjected to HiMC (B). (C,D) Relationship between myonuclear number and rpS6 content in individual myofibers from non-contracted legs (C) and legs subjected to HiMC (D). (E,F) Relationship between rpS6 and MPS in individual myofibers from non-contracted legs (E) and legs subjected to HiMC (F).

studies using immunoelectron microscopy and immunofluorescence previously reported the localisation of ribosomes near the perinuclear and z-bands (Galavazi and Szirmai, 1971; Larsen and Saetersdal, 1998), and our observations followed this. In addition, puromycin-labelled protein was also observed in sarcomere striation and perinuclear regions (Fig. 1B). This labelling pattern was similar to the known ribosome distribution. In a previous study, it was reported that *O*-propargyl puromycin-labelled protein localises along the sarcomere in the longitudinal muscle section (Liu et al., 2012), suggesting that protein synthesis occurred in the perinuclear and z-bands. Alternatively, puromycin-labelled proteins may accumulate around the perinuclear and z-bands. A recent study suggested that puromycin-labelled proteins are rapidly released from active ribosomes and do not necessarily accurately represent the site of protein synthesis (Enam et al., 2020). Thus, although our observations may not distinguish between the location of protein synthesis and the diffusion of synthetic proteins, the isolated muscle fibres used in the study seemed to maintain their overall morphological integrity.

TA subjected to acute HiMC displayed significantly elevated MPS (Fig. 2A,B). This response was consistent with our previous study (Ogasawara et al., 2016). Additionally, although we could not distinguish whether the labelling pattern of puromycin represented the site of translation or was more diffuse, the puromycin-derived fluorescence intensity was increased by HiMC without affecting the overall puromycin labelling pattern. The potential accurate localisation of the newly synthesised myofibrillar proteins and their location during muscle hypertrophy were recently discussed

Journal of Experimental Biology (2021) 224, jeb242496. doi:10.1242/jeb.242496

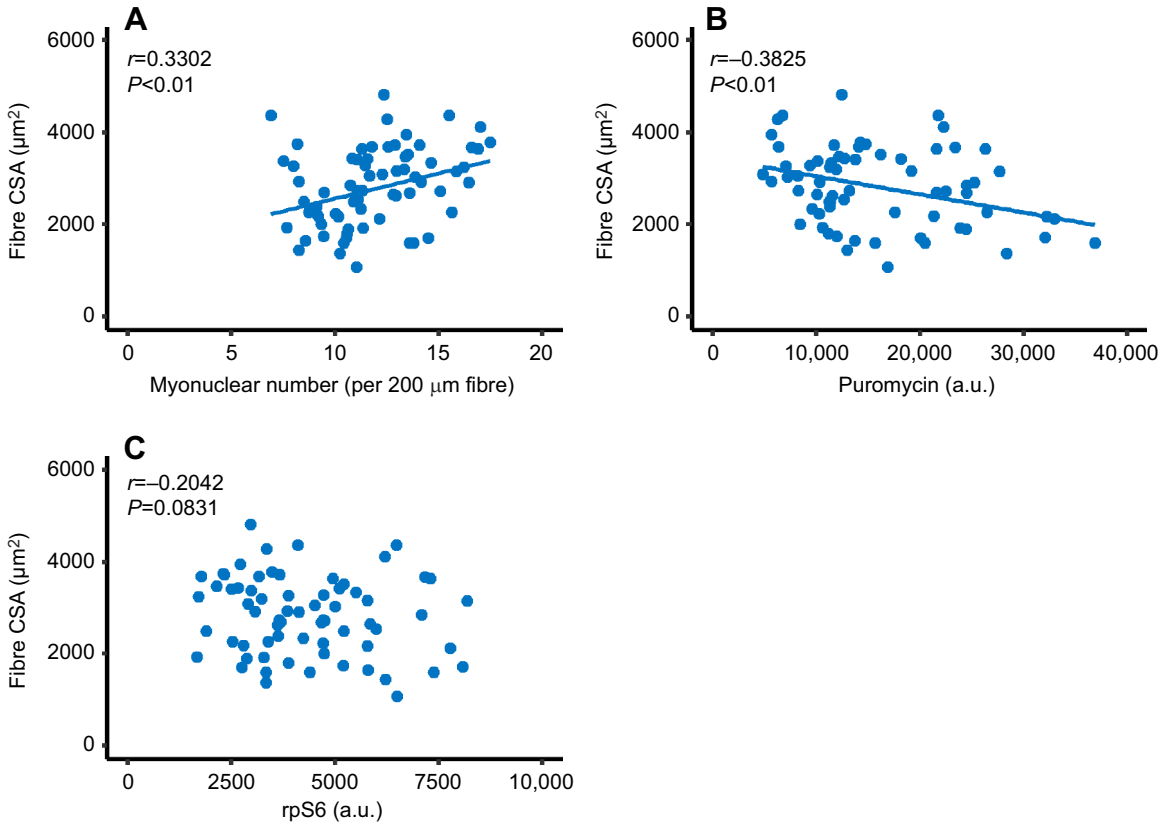

Fig. 4. Relationship between myofiber cross-sectional area (CSA) and number of myonuclei, ribosome content and MPS of individual muscle fibres under basal conditions. (A) Relationship between myonuclear number and myofiber CSA in individual myofibers. (B) Relationship between MPS and myofiber CSA in individual myofibers. (C) Relationship between rpS6 content and myofiber CSA in individual myofibers.

(Jorgenson et al., 2020). This point will be clarified using advanced techniques, such as click chemistry, in a future study. In addition, we counted the number of myonuclei using anti-PCM1 antibody (Winje et al., 2018). All nuclei were PCM1 positive, and the myonuclear number was unaffected by HiMC in this study (Fig. 3B). Thus, as in previous studies (Snijders et al., 2012), acute HiMC, such as resistance exercise, does not appear to cause changes in the number of myonuclei.

The role of multiple nuclei in skeletal muscle cells on muscle contraction-mediated hypertrophy has often been discussed (Bruusgaard et al., 2010; Damas et al., 2018; Gundersen, 2016; Petrella et al., 2008). In particular, as the nucleus is an important organelle for ribosome biosynthesis, myonuclear number has been considered to determine MPS capacity (Gundersen, 2016; Petrella et al., 2008). We observed that myonuclear number was slightly, but significantly, correlated with basal MPS (Fig. 3A; r=0.2852, P<0.01). There was also a significant correlation between rpS6 content and MPS in individual myofibers (Fig. 3E; r=0.5272, P<0.01). However, there was no association between myonuclear number and rpS6 content in individual muscle fibres (Fig. 3C; r=0.1813, P=0.1244). This suggests that factors other than ribosome content may underlie the correlation between myonuclear number and MPS in individual myofibers observed in resting skeletal muscle. The finding of a positive correlation between ribosome content and MPS in individual muscle fibres indicates that the positive association between ribosome content and resting MPS, observed in previous studies at the whole muscle level (Millward et al., 1973), is established at the level of a single muscle fibre as well.

In conditions of elevated MPS caused by HiMC, myonuclear number per unit fibre length was not corelated with MPS in individual muscle fibres (Fig. 3B; r=−0.0288, P=0.7925), while a positive correlation was observed between rpS6 content and MPS (Fig. 3E; r=0.4836, P<0.01). The present results indicate that the myonuclear number is uncoupled from the acute muscle contraction-related MPS capacity. However, the association between ribosome content and MPS was maintained even in myofibers where MPS was increased by contraction. Therefore, this suggests that ribosome content may be a determinant of MPS during early post-contraction recovery. However, this study did not directly evaluate ribosome content. Therefore, it may be necessary to evaluate this more accurately using alternative approaches, such as click chemistry (Kirby et al., 2016).

Here, we evaluated HiMC induced MPS at 6 h after recovery as the peak time; the increased MPS induced by HiMC in the form of, for example, resistance exercise, persists up to 48 h after the recovery of muscle contraction, and ribosome biogenesis occurs at the late (24 h) recovery phase (Ogasawara et al., 2016; Phillips et al., 1997; West et al., 2016). Given that the nucleus functions as the machinery for ribosome biogenesis, the relationship between the myonuclear number and MPS response due to muscle contraction might vary with the duration of recovery after an acute muscle contraction.

It has previously been observed that myonuclear number per unit fibre length is associated with individual muscle fibre size (Allen et al., 1995; Bruusgaard et al., 2003; Roy et al., 1999). Most recently, Cramer et al. (2020) have demonstrated at a causal level that the number of myonuclei is a limiting factor for the size of myofibers; it inhibits the fusion of myonuclei during growth of mice genetically

deficient in myonuclear fusion via *Mymk* gene knockout. However, they did not examine protein synthesis as a factor affecting cell size. In the present study, we observed a positive relationship between myonuclear number and fibre CSA, as in previous studies, and a weak correlation between myonuclear number and MPS. In contrast, fibre CSA was inversely correlated with MPS and there was no correlation with ribosome content. This suggests that factors other than ribosome content and MPS, such as the ability to supply mRNA as described by Millay's group (Cramer et al., 2020), may underlie the mechanism by which myonuclear number regulates growing muscle fibre size. For the myonuclear number–MPS–fibre CSA relationship, it is known that slow-twitch muscle fibres, which are smaller in CSA, have more nuclei and ribosomes, in addition to a higher MPS than fast-twitch muscle fibres, which are larger, and that there is a paradoxical relationship between the number of nuclei, MPS and muscle fibre size between different muscle fibre types (van Wessel et al., 2010). The present study suggests that there is a paradoxical relationship for the myonuclear number–MPS and MPS–fibre CSA even within TA, which is predominantly composed of fast-twitch (MHC type 2b is dominant) muscle fibres (Eng et al., 2008), although we were not able to classify the muscle fibre types.

Despite the fact that we were not able to investigate the relationship between myonucleus number, MPS and muscle fibre size under the conditions of increased muscle size because of chronic contraction, it is known that the increase in myonuclei and ribosomes associated with muscle contraction-induced hypertrophy is related to the degree of muscle hypertrophy (Ato et al., 2019; Nakada et al., 2016). It has also been observed during chronic resistance training in humans that the number of myonuclei per myofiber determined from transverse sections was strongly and positively correlated with post-exercise MPS, at the whole-muscle level (Damas et al., 2018). Thus, the myonuclear number–ribosome–MPS–myofiber size relationship may be dynamic under conditions of skeletal muscle size change, such as chronic contraction. These aspects need to be clarified in future studies.

Recently, myonuclei within a single muscle cell have been shown to transcriptionally and functionally branch at intracellular positions that include the myotendinous junction (MTJ) and/or the neuromuscular junction (NMJ) (Dos Santos et al., 2020; Perillo and Folker, 2018). These specific clusters of myonuclei were excluded from analysis in this study. However, it has previously been observed that some myonuclear populations in the cell body are localised along with the blood vessel (Ploug et al., 1998). Therefore, an unknown functional branch of the myonucleus other than the MTJ or NMJ may actively contribute to MPS or cell size regulation. Our understanding of the nature of the individual nuclei in skeletal muscle cells has only recently progressed. The detailed molecular regulation of the syncytial nature of skeletal muscle cells in terms of protein metabolism and cell size regulation should be clarified in the future.

Competing interests

The authors declare no competing or financial interests.

Author contributions

Conceptualization: S.A., R.O.; Methodology: S.A.; Validation: S.A.; Formal analysis: S.A.; Investigation: S.A., R.O.; Resources: S.A.; Data curation: S.A.; Writing - original draft: S.A., R.O.; Writing - review & editing: S.A., R.O.; Visualization: S.A.; Supervision: S.A.; Project administration: S.A.; Funding acquisition: S.A., R.O.

Funding

This work was supported by Japan Society for the Promotion of Science Grants-in-Aid for Scientific Research (KAKENHI) (19K19945 to S.A. and 19K22805 to R.O.) and Yamaha Motor Foundation for Sports.

References

Allen, D. L., Monke, S. R., Talmadge, R. J., Roy, R. R. and Edgerton, V. R. (1995). Plasticity of myonuclear number in hypertrophied and atrophied mammalian skeletal muscle fibers. *J. Appl. Physiol.* **78**, 1969-1976. doi:10.1152/jappl.1995.78.5.1969

Anthony, J. C., Yoshizawa, F., Anthony, T. G., Vary, T. C., Jefferson, L. S. and Kimball, S. R. (2000). Leucine stimulates translation initiation in skeletal muscle of postabsorptive rats via a rapamycin-sensitive pathway. *J. Nutr.* **130**, 2413-2419. doi:10.1093/jn/130.10.2413

Ato, S., Kido, K., Sato, K. and Fujita, S. (2019). Type 2 diabetes causes skeletal muscle atrophy but does not impair resistance training-mediated myonuclear accretion and muscle mass gain in rats. *Exp. Physiol.* **104**, 1518-1531. doi:10.1113/EP087585

Bruusgaard, J. C., Liestøl, K., Ekmark, M., Kollstad, K. and Gundersen, K. (2003). Number and spatial distribution of nuclei in the muscle fibres of normal mice studied in vivo. *J. Physiol.* **551**, 467-478. doi:10.1113/jphysiol.2003.045328

Bruusgaard, J. C., Johansen, I. B., Egner, I. M., Rana, Z. A. and Gundersen, K. (2010). Myonuclei acquired by overload exercise precede hypertrophy and are not lost on detraining. *Proc. Natl. Acad. Sci. U.S.A.* **107**, 15111-15116. doi:10.1073/pnas.0913935107

Cramer, A. A. W., Prasad, V., Eftestol, E., Song, T., Hansson, K.-A., Dugdale, H. F., Sadayappan, S., Ochala, J., Gundersen, K. and Millay, D. P. (2020). Nuclear numbers in syncytial muscle fibers promote size but limit the development of larger myonuclear domains. *Nat. Commun.* **11**, 6287. doi:10.1038/s41467-020-20058-7

Damas, F., Libardi, C. A., Ugrinowitsch, C., Vechin, F. C., Lixandrao, M. E., Snijders, T., Nederveen, J. P., Bacurau, A. V., Brum, P., Tricoli, V. et al. (2018). Early- and later-phases satellite cell responses and myonuclear content with resistance training in young men. *PLoS One* **13**, e0191039. doi:10.1371/journal.pone.0191039

Donaldson, S. K. (1984). Ca2+-activated force-generating properties of mammalian skeletal muscle fibres: histochemically identified single peeled rabbit fibres. *J. Muscle Res. Cell Motil.* **5**, 593-612. doi:10.1007/BF00713922

Dos Santos, M., Backer, S., Saintpierre, B., Izac, B., Andrieu, M., Letourneur, F., Relaix, F., Sotiropoulos, A., Maire, P. (2020). Single-nucleus RNA-seq and FISH identify coordinated transcriptional activity in mammalian myofibers. *Nat. Commun.* **11**, 5102. doi:10.1038/s41467-020-18789-8

Enam, S. U., Zinshteyn, B., Goldman, D. H., Cassani, M., Livingston, N. M., Seydoux, G. and Green, R. (2020). Puromycin reactivity does not accurately localize translation at the subcellular level. *eLife* **9**, e60303. doi:10.7554/eLife.60303

Eng, C. M., Smallwood, L. H., Rainiero, M. P., Lahey, M., Ward, S. R. and Lieber, R. L. (2008). Scaling of muscle architecture and fiber types in the rat hindlimb. *J. Exp. Biol.* **211**, 2336-2345. doi:10.1242/jeb.017640

Galavazi, G. and Szirmai, J. A. (1971). The influence of age and testosterone on the ribosomal population in the m. levator ani and a thigh muscle of the rat. *Zeitschrift für Zellforschung und Mikroskopische Anatomie* **121**, 548-560. doi:10.1007/BF00560159

Goodman, C. A., Frey, J. W., Mabrey, D. M., Jacobs, B. L., Lincoln, H. C., You, J.-S. and Hornberger, T. A. (2011a). The role of skeletal muscle mTOR in the regulation of mechanical load-induced growth. *J. Physiol.* **589**, 5485-5501. doi:10.1113/jphysiol.2011.218255

Goodman, C. A., Mabrey, D. M., Frey, J. W., Miu, M. H., Schmidt, E. K., Pierre, P. and Hornberger, T. A. (2011b). Novel insights into the regulation of skeletal muscle protein synthesis as revealed by a new nonradioactive in vivo technique. *FASEB J.* **25**, 1028-1039. doi:10.1096/fj.10-168799

Gundersen, K. (2016). Muscle memory and a new cellular model for muscle atrophy and hypertrophy. *J. Exp. Biol.* **219**, 235-242. doi:10.1242/jeb.124495

Hall, Z. W. and Ralston, E. (1989). Nuclear domains in muscle cells. *Cell* **59**, 771-772. doi:10.1016/0092-8674(89)90597-7

Jorgenson, K. W., Phillips, S. M. and Hornberger, T. A. (2020). Identifying the Structural Adaptations that Drive the Mechanical Load-Induced Growth of Skeletal Muscle: A Scoping Review. *Cells* **9**, 1658. doi:10.3390/cells9071658

Kirby, T. J., Patel, R. M., McClintock, T. S., Dupont-Versteegden, E. E., Peterson, C. A. and McCarthy, J. J. (2016). Myonuclear transcription is responsive to mechanical load and DNA content but uncoupled from cell size during hypertrophy. *Mol. Biol. Cell* **27**, 788-798. doi:10.1091/mbc.E15-08-0585

Konigsberg, U. R., Lipton, B. H. and Konigsberg, I. R. (1975). The regenerative response of single mature muscle fibers isolated *in vitro*. *Dev. Biol.* **45**, 260-275. doi:10.1016/0012-1606(75)90065-2

Larsen, T. H. and Saetersdal, T. (1998). Translocation of 60S ribosomal subunit in spreading cardiac myocytes. *J. Histochem. Cytochem.* **46**, 963-970. doi:10.1177/002215549804600810

Lepper, C., Partridge, T. A. and Fan, C. M. (2011). An absolute requirement for Pax7-positive satellite cells in acute injury-induced skeletal muscle regeneration. *Development* **138**, 3639-3646. doi:10.1242/dev.067595

Liu, J., Xu, Y., Stoleru, D. and Salic, A. (2012). Imaging protein synthesis in cells and tissues with an alkyne analog of puromycin. *Proc. Natl. Acad. Sci. U.S.A.* **109**, 413-418. doi:10.1073/pnas.1111561108

Millward, D. J., Garlick, P. J., James, W. P. T., Nnanyelugo, D. O. and Ryatt, J. S. (1973). Relationship between Protein Synthesis and RNA Content in Skeletal Muscle. *Nature* **241**, 204. doi:10.1038/241204a0

Morkin, E. (1970). Postnatal muscle fiber assembly: localization of newly synthesized myofibrillar proteins. *Science* **167**, 1499-1501. doi:10.1126/science.167.3924.1499

Nakada, S., Ogasawara, R., Kawada, S., Maekawa, T. and Ishii, N. (2016). Correlation between ribosome biogenesis and the magnitude of hypertrophy in overloaded skeletal muscle. *PLoS One* **11**, e0147284. doi:10.1371/journal.pone.0147284

Ogasawara, R., Fujita, S., Hornberger, T. A., Kitaoka, Y., Makanae, Y., Nakazato, K. and Naokata, I. (2016). The role of mTOR signalling in the regulation of skeletal muscle mass in a rodent model of resistance exercise. *Sci. Rep.* **6**, 31142. doi:10.1038/srep31142

Perillo, M. and Folker, E. S. (2018). Specialized positioning of myonuclei near cell-cell junctions. *Front Physiol* **9**, 1531. doi:10.3389/fphys.2018.01531

Petrella, J. K., Kim, J. S., Mayhew, D. L., Cross, J. M. and Bamman, M. M. (2008). Potent myofiber hypertrophy during resistance training in humans is associated with satellite cell-mediated myonuclear addition: a cluster analysis. *J. Appl. Physiol.* **104**, 1736-1742. doi:10.1152/japplphysiol.01215.2007

Phillips, S. M., Tipton, K. D., Aarsland, A., Wolf, S. E. and Wolfe, R. R. (1997). Mixed muscle protein synthesis and breakdown after resistance exercise in humans. *Am. J. Physiol.* **273**, E99-E107. doi:10.1152/ajpendo.1997.273.1.E99

Ploug, T., van Deurs, B., Ai, H., Cushman, S. W. and Ralston, E. (1998). Analysis of GLUT4 distribution in whole skeletal muscle fibers: identification of distinct storage compartments that are recruited by insulin and muscle contractions. *J. Cell Biol.* **142**, 1429-1446. doi:10.1083/jcb.142.6.1429

Ravi, V., Jain, A., Ahamed, F., Fathma, N., Desingu, P. A. and Sundaresan, N. R. (2018). Systematic evaluation of the adaptability of the non-radioactive SUnSET assay to measure cardiac protein synthesis. *Sci. Rep.* **8**, 4587. doi:10.1038/s41598-018-22903-8

Roy, R. R., Monke, S. R., Allen, D. L. and Edgerton, V. R. (1999). Modulation of myonuclear number in functionally overloaded and exercised rat plantaris fibers. *J. Appl. Physiol.* **87**, 634-642. doi:10.1152/jappl.1999.87.2.634

Sambasivan, R., Yao, R., Kissenpfennig, A., Van Wittenberghe, L., Paldi, A., Gayraud-Morel, B., Guenou, H., Malissen, B., Tajbakhsh, S. and Galy, A. (2011). Pax7-expressing satellite cells are indispensable for adult skeletal muscle regeneration. *Development* **138**, 3647-3656. doi:10.1242/dev.067587

Schmidt, E. K., Clavarino, G., Ceppi, M. and Pierre, P. (2009). SUnSET, a nonradioactive method to monitor protein synthesis. *Nat. Methods* **6**, 275-277. doi:10.1038/nmeth.1314

Snijders, T., Verdijk, L. B., Beelen, M., McKay, B. R., Parise, G., Kadi, F. and van Loon, L. J. (2012). A single bout of exercise activates skeletal muscle satellite cells during subsequent overnight recovery. *Exp. Physiol.* **97**, 762-773. doi:10.1113/expphysiol.2011.063313

Snijders, T., Smeets, J. S., van Kranenburg, J., Kies, A. K., van Loon, L. J. and Verdijk, L. B. (2016). Changes in myonuclear domain size do not precede muscle hypertrophy during prolonged resistance-type exercise training. *Acta Physiol* **216**, 231-239. doi:10.1111/apha.12609

Thomson, E., Ferreira-Cerca, S. and Hurt, E. (2013). Eukaryotic ribosome biogenesis at a glance. *J. Cell Sci.* **126**, 4815-4821. doi:10.1242/jcs.111948

van Wessel, T., de Haan, A., van der Laarse, W. J. and Jaspers, R. T. (2010). The muscle fiber type-fiber size paradox: hypertrophy or oxidative metabolism? *Eur. J. Appl. Physiol.* **110**, 665-694. doi:10.1007/s00421-010-1545-0

West, D. W., Baehr, L. M., Marcotte, G. R., Chason, C. M., Tolento, L., Gomes, A. V., Bodine, S. C. and Baar, K. (2016). Acute resistance exercise activates rapamycin-sensitive and -insensitive mechanisms that control translational activity and capacity in skeletal muscle. *J. Physiol.* **594**, 453-468. doi:10.1113/JP271365

Winje, I. M., Bengtsen, M., Eftestol, E., Juvkam, I., Bruusgaard, J. C. and Gundersen, K. (2018). Specific labelling of myonuclei by an antibody against pericentriolar material 1 on skeletal muscle tissue sections. *Acta Physiol* **223**, e13034. doi:10.1111/apha.13034

You, J. S., Anderson, G. B., Dooley, M. S. and Hornberger, T. A. (2015). The role of mTOR signaling in the regulation of protein synthesis and muscle mass during immobilization in mice. *Dis Model Mech* **8**, 1059-1069. doi:10.1242/dmm.019414